Breakdown Phenomena of a Vacuum Interrupter after Current Zero

Lionel R. Orama
General Engineering Department
University of Puerto Rico, Mayagüez
Mayagüez, Puerto Rico 00681-9044
lorama@ece.uprm.edu

Abstract - **A study on breakdown phenomena in a vacuum interrupter was conducted with the use of a numerical model based on the continuous transition model by Andrews and Varey [1]. The vacuum model was validated against test data for the device under consideration. The study aim to find the mechanisms that prompt the breakdown of the interrupter as well as interrupting limits for the specified device under critical power system conditions. It was observed that the peak of the electric field over the new cathode, after current zero, occurs typically during the first three to four microseconds of the post-arc period on the examined device. Although the recovery voltage is still increasing at the time, the early peak happens due to approximately 50% decay on the density of ions in the sheath that develops in front of the electrode. Despite the pre-breakdown observed close to the peak of the electric field, the breakdown never precipitated. In tests where breakdown occurred, it was also observed a pre-breakdown close to the peak of the power density at the new cathode after current zero. A few tens of a microsecond after the occurrence of the power density peak, the complete breakdown of the vacuum took place. Since both mechanisms were present, it was concluded that the breakdown in the studied devices was a consequence of a combination of mechanisms, due to what is known as thermionic-field emissions.**

Keywords: Vacuum interrupters, breakdown phenomena, anode/cathode phenomena.

I. INTRODUCTION

The period after current zero, known as the post-arc period, is critical for the interruption process in vacuum switches. In vacuum a pause of several to tens of nanoseconds exists between the current zero crossing and the beginning of the transient recovery voltage (TRV) [2, 3, 4]. Fig. 1 helps to describe the phenomena in the inter-electrode space around current zero (CZ). The current density through the plasma is described as,

$$J = n_e q_e v_e + n_i q_i v_i Z \qquad (1)$$

where,
n_e and n_i are the electron and ion densities
q_e and q_i are the electron and ion charges ($q_e = e$)
v_e and v_i are the electron and ion velocities
Z is the ion charge multiplicity constant.
Assuming a quasi-neutral plasma, and that the ions and electrons travel in the same direction, to the anode, (1) becomes,

$$J = n\left(ev_e + \left(-Ze\right)v_i\right) = ne\left(v_e - Zv_i\right) \qquad (2)$$

Before CZ v_e is higher than Zv_i, but v_e is decreasing, so the current is decreasing to zero. Since, the electron mass is several orders of magnitude smaller than the ion's (electron mass = 9.11×10^{-31} kg, Cu ion mass = 1.056×10^{-25} kg), it can be assumed that the velocity of the ions remains almost constant. At the instant of CZ the v_i and Zv_e are equal, and therefore $J = 0$.
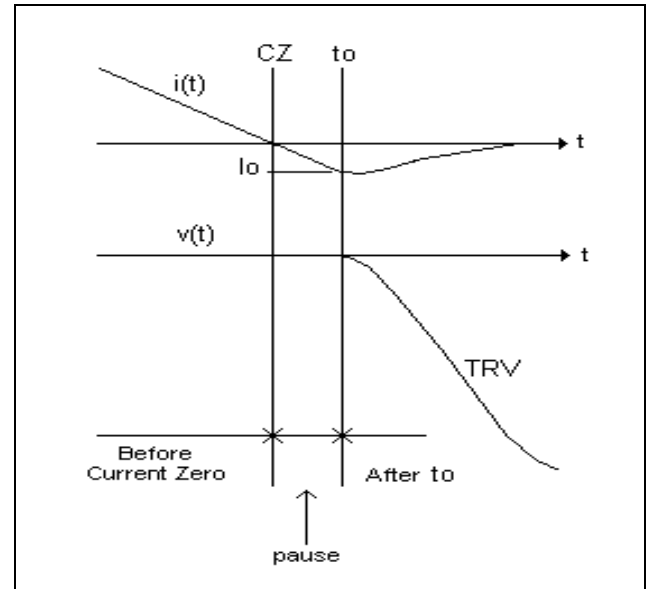
Fig 1 Current zero phenomena in a vacuum interrupter.

After CZ, v_e continues to decrease until an instant when it reaches zero. This period continues from CZ to t_0. After the instant t_0 the electrons reverse their direction, now from the anode (new cathode after CZ) to the cathode (new anode after CZ). They accelerate and start leaving a sheath of positive ions behind, in front of the anode (new cathode after CZ) [3]. At this point the voltage (TRV) starts developing across the positive ion sheath. This time marks the beginning of the interruption process in the vacuum device (I_0 at t_0 in fig. 1).

The electric field that develops across the ion sheath depends on the voltage, the ion density in the sheath, and other post arc plasma parameters. In addition, since the ions travel to the new cathode, they collide with the new cathode surface thus transferring energy to the surface. Both of these phenomena have the potential to cause the

breakdown of the ion sheath when they either increase too fast or reach high magnitudes.

In this paper, the author attempts to explain these breakdown phenomena in the light of the simulation results, and compare them with the tests of actual vacuum devices.

II. ELECTRICAL AND THERMAL-LIKE BREAKDOWN DURING POST ARC PERIOD

If the electric field reaches a sufficiently high magnitude, electrons will be emitted from the surface of the metal into the ion sheath. This can cause collisions with other species and eventually a breakdown [5]. Also, if the electrode temperature increases in excess of 1480°C for Cu, for instance, due to the ion bombardment, a breakdown will follow [5, 6].

Two sets of tests were received from Edward Huber, Technical University of Vienna [7]. Both sets were performed for the same device under different electrical system conditions. Testing conditions can be found in table 1. In table 2 the model parameters for simulation of each test are listed. These parameters were found using a parameter extraction and optimization program developed by the author using MATLAB [1, 8]. The following section will present the simulation results of the devices from table 1 and the analysis of the breakdown mechanisms.

test series	gap mm	Irms kA	TRV kV	Comments
1	6.5	25	70	full arcing time
2	10.0	40	55	full gap

Table 1 Test conditions for vacuum interrupters from reference [7].

test series	gap mm	N_{i0} $x10^{20}m^{-3}$	AMP	tau μs	v_i m/s	D_0 mm
1	6.5	2.2	1.329	5.17	2250	5.0
2	10.	4.37	1.447	4.09	1000	5.3

Table 2 Vacuum model parameters extracted from the tests of table 4.1. Simulation results compared to tests

A. Simulation Results Compared to Test

The phenomena presented in the test oscillograms will be analyzed with the help of the simulation results and explained qualitatively. Fig. 2 presents a representative sample of traces from series #1. The first and second plots show the TRV and post arc current (Ipa) traces for both simulation and test. The third plot shows the computed field on the anode surface (new cathode after CZ). It is interesting to notice the period from point *a* to *b* on the figure. A pre-breakdown occurs during this period (instability of current and voltage at $\cong 4.6\mu$s). It coincides

with the peak of the electric field (62.2MV/m). In this test the interrupter recovers and the breakdown does not precipitate. The peak electric field happens approximately 3μs before the peak of the TRV. This can be explained since, the electric field is not a function of the voltage
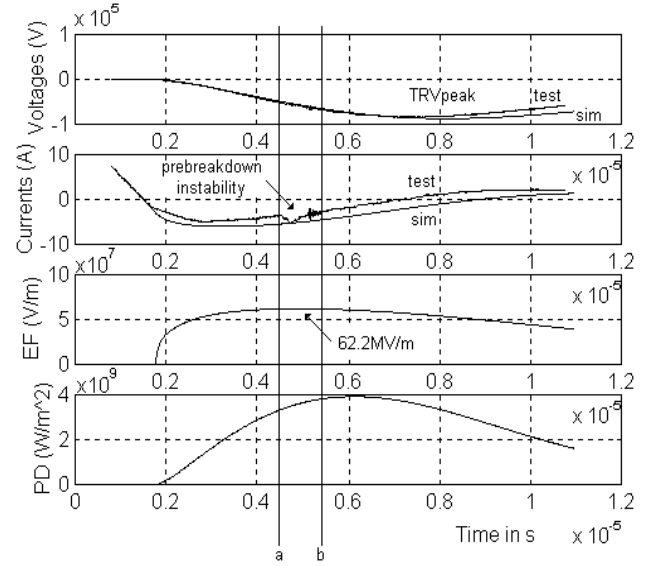
Fig. 2 Vacuum interrupter from test series #1 under pre-breakdown due to the electric field.

across the ion sheath alone. Fig. 3 indicates a decay from $1.5x10^{20}$ to $0.8x10^{20}m^{-3}$ on the ion density at the sheath edge (N_i), the plasma potential (U_0) remaining approximately constant (1.62-1.67V). Since the electric field is a function of the *TRV*, N_i and U_0, the combination of N_i and the *TRV* is the likely agent responsible for the early peak.

The simulation results of sample test #2 are displayed in fig. 4. A pre-breakdown is visible at 9.5μs (at 70.8MV/m, E_{peak}=75MV/m), before the electric field reaches its maximum. The instability of the pre-breakdown does not lead to a full breakdown of the gap. However, in this picture the instability lasts longer (4.5μs) than in fig. 2, most likely as a consequence of the higher electric field. Notice also that at 11.6μs another instability occurs. The latter occurs at the peak of the power density distribution (PD) of $4.9x10^9$W/m^2, and probably reflects the "thermal-like" mechanism.

None of the cases examined, including test series not shown, exhibits a breakdown of the gap that was an extension of the first field breakdown instability alone. It would be expected that around the peak of the electric field the breakdown occurred as a direct consequence of the first instability. This suggests that in the tests studied there were no pure electric field breakdowns or the breakdown was associated with combination of mechanisms. This is in spite of the fact that the computed electric field was high, ranging from 60 to 75MV/m.
On the other hand, the results indicate that an electric field pre-breakdown activity happens early in the interruption

process, when the electric field and TRV are rising or are at their peak value. During this period the ion density at the sheath is high and the sheath length is just beginning to develop (short effective gap).
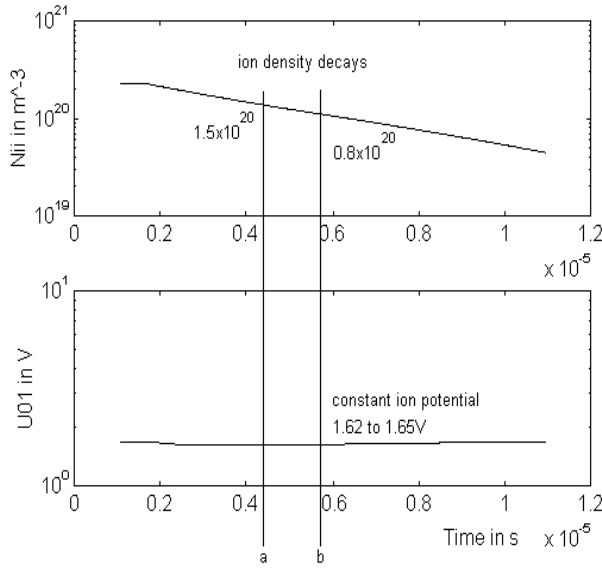
Fig. 3 Ion density and potential at the sheath, for vacuum interrupter in test series #1.
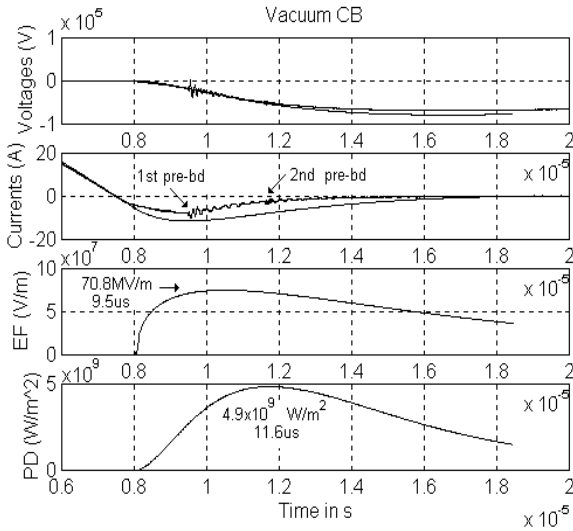
Fig. 4 Vacuum interrupter from test series #2 under pre-breakdown due to electric field and power density.

The next figure from another test in test series #1 reveals other details. There is a visible instability in the traces of current and voltage in fig. 5, at the peak of the electric field, between 5 and 5.5μs. The instability does not precipitate, but roughly 1μs later, at 6.5μs, a sudden pre-breakdown occurs, 0.4μs after the peak of the power density ($3.9x10^9$MW/m^2 at 6.1μs). Afterwards, the complete breakdown of the device results at 7.7μs. Since, the first pre-breakdown vanishes completely before the second one, the plots suggest that in this case the thermal mechanism (power density) has greater effect on the breakdown than

the electric field. One can also speculate that the delay between the peak of the PD and the breakdown results from an accumulation of heat on the ion-bombarded anode (new cathode). Fig. 6 also exhibits this behavior. A minor pre-breakdown occurs at the peak of the electric field (62.2MV/m at 5μs). This instability diminishes and completely disappears.
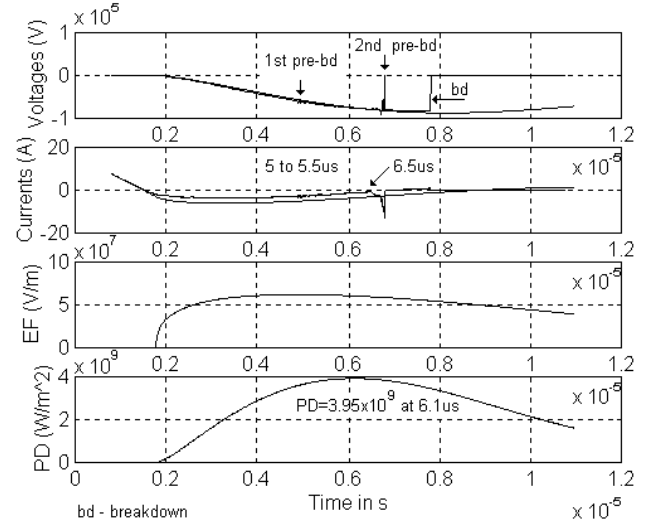
Fig. 5 Vacuum interrupter from test series #1 under pre-breakdown due to an electric field and power density followed by a failure of the gap.

Then, 0.6μs after the peak of the power density, a sudden breakdown of the gap follows at 6.8μs. Fig. 7 from test series #2 displays a small instability that diminishes from 12.5 to 13μs, but never clears completely. This pre-breakdown occurs 0.65μs after the peak of the power density. Finally, the instability amplifies after 14μs, ending in the total breakdown of the gap at 19μs. When the instability amplifies the value of the electric field still remains over 60MV/m.

The evidence presented suggests that for the cases under consideration (test series #1 and #2) the mechanism that dominates the failure of the interrupter was a thermal-like breakdown. In the next sections the author presents other numerical models to describe the physics of the thermal phenomena on the surface of the electrode under such circumstances and calculates possible temperatures due to the ion bombardment.

B. Conduction heat transfer at the anode due to ion bombardment

When studying the breakdown after current zero in vacuum devices, it is of interest to know the heat transfer response at the electrode/vacuum interface. The principle mechanism of heat transfer is conduction into the contact material. Radiation to the surroundings is negligible [6, 9, 10]. The present section describes a model for conduction heat transfer, and the results of simulation of the thermal

conduction in the Cu electrodes under transient conditions similar to the post-arc current region.
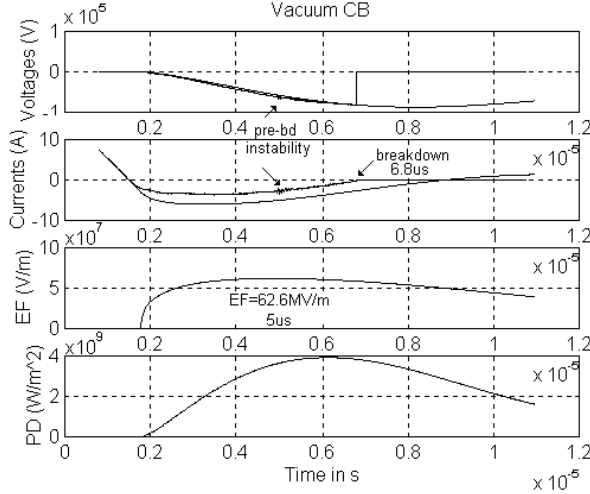
Fig. 6 Vacuum interrupter from test series #1 under pre-breakdown due to an electric field followed by a failure of the gap, possibly due to power density.

A routine was developed in MATLAB to simulate the heat transfer in the solid Cu surface when a source of energy is applied. Carslaw & Jaeger [11], and Ingersoll, et al [12] solved the equation of heat conduction by the method of sources and sinks. The solution for a continuous point source over a semi-infinite solid surface is,

$$T(r,t) = \frac{1}{8(pa)^{\frac{3}{2}}} \int_0^t \frac{f(t')e^{\frac{-r^2}{4a(t-t')}}}{(t-t')^{\frac{3}{2}}} \cdot dt' \quad (3)$$

$$a = \frac{k}{rc} \quad (4)$$

where,
a, is the diffusivity constant of the solid material
k, is the thermal conductivity constant of the solid, 385W/m² °C for Cu
r, is the density of the material, 8.89x10⁶ g/m³ for Cu
c, is the specific heat of the material, 0.386 J/g °C for Cu
t, is time in seconds
T is the temperature in °C
r, is the radius of the spherical shell of interest in meters, and
$f(t)$, is a time dependent heat source function.

Equation 3 describes the temperature change in the semi-infinite solid as a function of time, position, and the thermal characteristics of the solid material. The integrand of the equation was numerically computed using the function *quad8* within MATLAB [1, 8].

The input source $f(t)$ used for the simulation was the same power density PD as calculated from the interrupter's

simulation [1]. In order to use the power density function it was first approximated by a polynomial using the *polyfit* routine in MATLAB [1, 8]. Fig. 8 displays
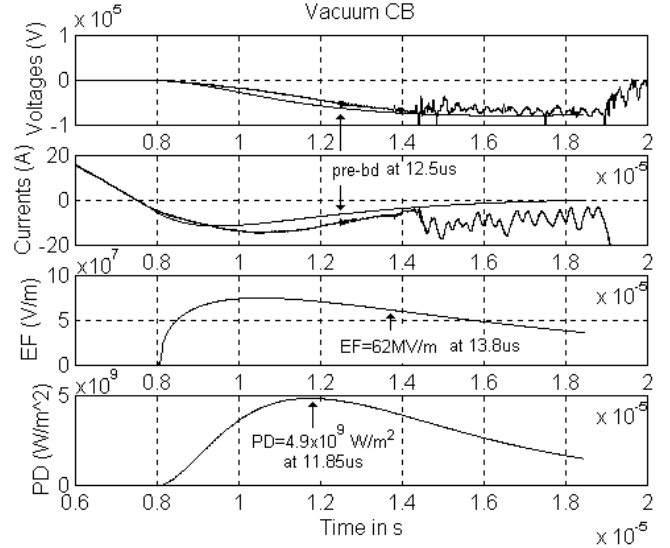
Fig. 7 Vacuum interrupter from series test #2 under pre-breakdown due to power density followed by a failure of the gap, possibly due to both electric field and power density.

the time distribution of the temperature change over different concentric hemispherical layers inside the electrode, for test series #1. The heat wave arrives with a different time delay for different radii shown (2.5μm at 6.97μs, at 5μm at 7.05μs, 10μs at 7.39μs, at 15μs at 7.78μs). It is important to note that due to this traveling wave, the peak temperatures in the layers occur after the peak of the power density (3.92MW/m² at 6.14μs). Also, the magnitude of the temperature change is of importance. The simulation shows that the change in temperature ranges from 250°C at 15μm to 655°C at 2.5μm, under the thermal stress imposed by ion bombardment after current zero.

These simulation results suggest that breakdowns occurring in the device under study result from the thermal mechanism, because the peak of the power density occurs just before the peak of the TRV and there is a delay in the temperature increase over the electrode. The results in fig. 8 are in good agreement with the earlier predictions reported by Glinkowski [4].

C. Anode power density and surface temperature prior to current zero.

In this section the possible temperatures of the anode surface during arcing and at CZ are computed. An approximate value of the surface temperature at CZ helps to estimate how the ion bombardment after CZ can bring this surface temperature to the boiling point and cause a breakdown.

For Cu electrodes in diffuse vacuum arcs the arcing voltage range from 20 to 40V. Assuming a constant arc voltage, and

that the current collected is uniformly distributed over the anode surface prior to current zero
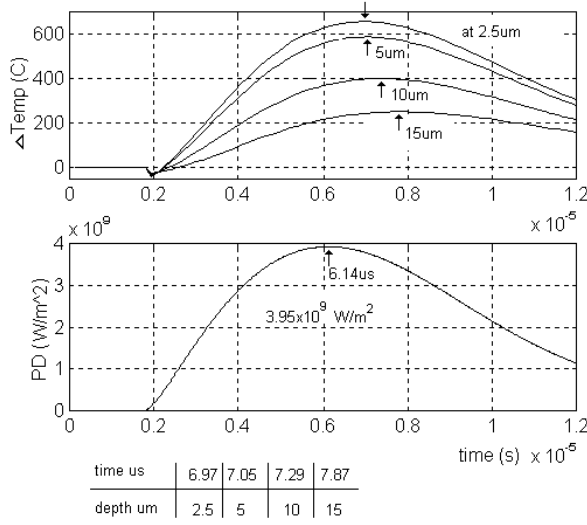
Fig. 8 Thermal response of a semi-infinite Cu electrode after current interruption. The power density used was taken from test series #1, figure 4.2 the test with lowest PD_{peak}.

(diffuse arc), the power density can be found by

$$Pd = Pd_{peak} \sin(\omega t) = \frac{I_t V_{arc}}{A} \sin(\omega t) \qquad (5)$$

I_t, is the 50Hz peak current of the test (test series #1 or #2)
V_{arc}, is the arcing voltage
A, is the area of the electrode surface (radius 30mm)
ω, is the power system frequency ($2\pi(50Hz)$).

The computed peak power densities for the test conditions in table 1 are shown in the table 3. Equation 5 was used as the input source for the solution of the heat conduction equation of a cylindrical surface [11, 12]. This conduction equation was solved by the same approach used for equation 3 in section B. The surface temperature is presented on fig. 9, for a power density of $50 \times 10^7 W/m^2$.
Assuming a cold electrode at the beginning of the simulation, fig. 9 shows that the temperature at CZ

Test number	Current KA_{rms}	Voltage V	Pd_{peak} $x10^7 W/m^2$
1	25	25	31.3
1	25	40	50.0
2	40	25	50.0
2	40	40	80.0

Table 3 Approximate peak power densities of device in test series # 1 and #2

reaches 718°C. This value is the approximate initial temperature of the anode when the interruption process begins.

D. Electron emission due to power density and electric field.

With the results presented in sections B and C the calculation of the thermionic emission and the thermionic-field emission of electrons to the ion sheath can be found. From reference [13] the equation for the thermionic emission is,

$$J_t = AT_0^2 e^{-\frac{q f}{kT_0}} \qquad (6)$$

where,
A, is a constant for the material, 65A/cm^{2}K^2 for Cu
T_0, is the temperature of the emitter when the electric field is zero
q, is the electron charge
f, is the work function of the material, 4.5eV for Cu, and
k, is the Boltzmann's constant (8.62e-5eV/K).
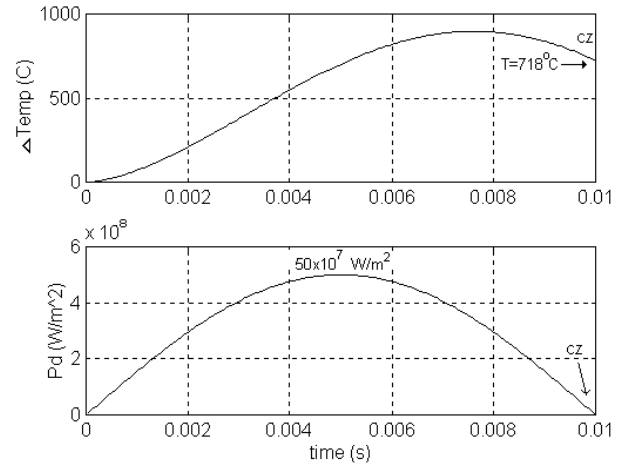
Figure 9 Surface temperature of the anode during full arcing period of test one (upper trace). Lower trace, power density due to steady arc, prior to current zero. Radius of cylindrical contact equals 30mm.

The Schottky emission theory [5, 13, 14] establishes that when a heated electrode is exposed to an electric field (E) the work function of the electrode material is modified as,

$$f_{eff} = f - \sqrt{qE} \qquad (7)$$

and is called the "effective" work function. Equation 7 is substituted into 6 to obtain the field-enhanced thermionic emision current density,

$$J_{tf} = AT^2 e^{-\left(\frac{q\left(f - \sqrt{qE}\right)}{kT}\right)} \qquad (8)$$

For a Cu emitter, if E is expressed in Volts/cm equation 8 becomes [13]

$$J_{tf} = J_0 e^{\frac{4.389\sqrt{E}}{T}} \qquad (9)$$

where J_0 is the thermionic emission from equation 6. Equation 9 expresses the current density (J_{tf}) from the surface of an electrode that has been subjected to both thermal and electric fields.

Equation 9 was solved using the temperatures from the preceding sections (B & C) and with the electric field calculated interrupter's simulation of test series #1. Fig. 10 shows how J_{tf} changes due to the thermionic-field emission as compared with the J_t due to the thermionic
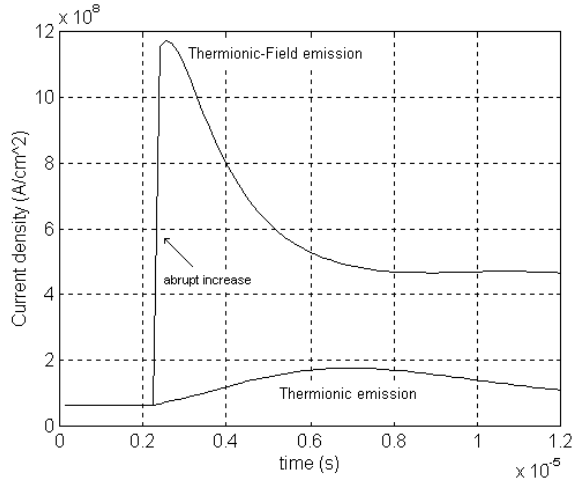
Fig. 10 Current density due to thermionic and thermionic-field emissions, for test series #1.

emission only. An abrupt increase in the J_{tf} is shown, between 2 and 3μs. This sudden increase is due to the fast rise of the electric field as seen in figures 2, 5, and 6. Although the electric field stays almost constant from 4 to 6μs the temperature continues increasing, therefore, the argument of the exponetial function decreases (equation 9) and the current density decreases. After the temperature reaches its peak (at 7μs) the current density remains almost constant, because both the electric field and the temperature starts decreasing. The behavior of the J_{tf} agrees with the Schottky thermionic-field emission theory. The current density (J_{tf}) reaches a value of the order of 10^8A/cm^2, which is comparable to a density inside a cathode spot.

III. CONCLUSIONS

The peak of the electric field over the new cathode occurs typically during the first 3 to 4μs of the post-arc period, for the tested devices. Although the recovery voltage is still increasing, this early peak happens due to decay of the ion density in the sheath. At this time the ion sheath is very short (<1mm). Since the sheath length is the effective gap of the vacuum device, this short length in combination with the high electric field could generate a breakdown [4].

During the post arc period the traveling ions collide with the surface of the cathode. It has been demonstrated that ion bombardment can elevate the surface temperature and consequently the vapor pressure in the interelectrode space. With the aid of the electric field at the cathode surface, breakdown of the ion sheath can follow. Under the tested conditions, the vacuum interrupters failed not as a consequence of the electric filed alone, but by the combined effect of electric field and temperature rise.

VI. REFERENCES

[1] L. R. Orama, "Numerical Modeling of High Voltage Circuit Breaker Arcs and their Interaction with the Power System", Ph.D. Thesis, Rensselaer Polytechnic Institute, Troy, NY, October 1997.

[2] S. Childs, A. Greenwood, J. Sullivan, "Events Associated with Current Zero Passage during the Rapid Commutation of Vacuum Arc", IEEE Trans. Palsma Sci., Vol. PS-11, No. 3, Sept 1983, pp. 181-188.

[3] M.T. Glinkowski, A. Greenwood, "Some Interruption Criteria for Short High Frequency Vacuum Arcs", IEEE Trans. Plasma Sci., Vol. PS-17, No. 5, Oct 1989, pp. 741-743.

[4] M.T. Glinkowski, "Behavior of Vacuum Switching Devices for Short Gaps", Ph.D. Thesis, Rensselaer Polytechnic Institute, Troy, NY, December 1989.

[5] J.M. Lafferty (Editor), Vacuum Arcs-Theory and Application, John Wiley & Sons, NY, 1980.

[6] G.R. Mitchell, L.P. Harris, "The Structure of Vacuum Arcs and the Design of Vacuum Interrupters", Conference Paper C75 067-4, IEEE PES Winter Meeting, NY, January 1975.

[7] E. Huber, Private Communication, 1996.

[8] MATLAB: High Performance Numeric Computation and Visualization Software, Reference Guide, The Math Works, September 1994.

[9] C.W. Kimblin, "Anode Voltage Drop and Anode Spot Formation in DC Vacuum Arcs", Journal of Applied Physics, Vol. 40, No. 4, March 1969, pp. 1644-1752.

[10] F.M. Charbonnier, C.J. Bennette, L.W. Swanson, "Electrical Breakdown Between Metal Electrodes in High Vacuum, I. Theory", Journal of Applied Physics, Vol. 38, No.2, February 1967, pp. 627-633.

[11] H.S. Carslaw, J.C. Jaeger, Conduction of Heat in Solids, Clarendon Press, Oxford, 1959.

[12] L.R. Ingersoll, O.J. Zobel, A.C. Ingersoll, Heat Conduction with Engineering, Geological and Other Applications, The University of Wisconsin Press,

Wisconsin, 1954.

[13] J.D. Cobine, <u>Gaseous Conductors</u>, Mc Graw-Hill , NY, 1941.

[14] W. Schottky, Z. Phys., Vol. 14, No. 63, 1923.